Magnetic transition in a correlated band insulator

A. Euverte, S. Chiesa, R. T. Scalettar, and G. G. Batrouni

Magnetic transition in a correlated band insulator

A. Euverte[1], S. Chiesa[2], R.T. Scalettar[3], and G.G. Batrouni[1,4]

[1]*INLN, Université de Nice-Sophia Antipolis, CNRS; 1361 route des Lucioles, 06560 Valbonne, France*
[2]*Department of Physics, College of William & Mary, Williamsburg, VA 23185, USA*
[3]*Physics Department, University of California, Davis, California 95616, USA and*
[4]*Institut Universitaire de France*

The effect of on-site electron-electron repulsion U in a band insulator is explored for a bilayer Hubbard Hamiltonian with opposite sign hopping in the two sheets. The ground state phase diagram is determined at half-filling in the plane of U and the interplanar hybridization V through a computation of the antiferromagnetic (AF) structure factor, local moments, single particle and spin wave spectra, and spin correlations. Unlike the case of the ionic Hubbard model, no evidence is found for a metallic phase intervening between the Mott and band insulators. Instead, upon increase of U at large V, the behavior of the local moments and of single-particle spectra give quantitative evidence of a crossover to a Mott insulator state preceeding the onset of magnetic order. Our conclusions generalize those of single-site dynamical mean field theory, and show that including interlayer correlations results in an increase of the single particle gap with U.

PACS numbers: 71.10.Hf, 71.27.+a, 02.70.Uu

Introduction: Whether interactions might drive metallic behavior in two dimensional disordered systems, where disorder just marginally succeeds in localizing all the eigenstates, is a question that has been the subject of considerable experimental and theoretical scrutiny[1–3]. It is natural to ask the same question concerning band insulators which likewise have vanishing dc conductivity in the absence of interactions. In the case of band insulators, carrier density plays an especially central role, since the band must be precisely filled. This lends an additional complexity to the issue, since interactions might also give rise to Mott insulating and magnetic behavior.

The possible connection between disordered interacting systems, and correlated band insulators is made more concrete by considering the Anderson model, where random site energies couple to the local density, and the 'ionic' Hubbard model (IHM)[4] which has a superlattice potential where the site energy has a regular structure, taking two distinct values on the sublattices of a bipartite lattice. On the one hand, it is plausible that the same physical effects that could cause a metallic transition for random site energies, the reduction of charge inhomogeneity and resulting delocalization of the electronic wave functions by interparticle repulsion, would also be operative in the patterned case. On the other hand, momentum is still a good quantum number in the presence of a regular array of site energies, suggesting possible differences between the effect of U in the two situations.

The approximations made in the most simple, single site, Dynamical Mean Field Theory (DMFT) approach[5] to the treatment of electron-electron interaction emphasize some of the possible nuances in attempting to elucidate the physics of correlated band insulators. Single site DMFT can capture the band insulator (and how it differs from an Anderson insulator) by incorporating a density of states with $N(E_\mathrm{F}) = 0$. However, it also minimizes the role of momentum, and hence blurs some of the distinction between band and Anderson insulators.

DMFT has, in fact, been used to explore whether correlations can drive a band insulator metallic. Garg *et al.* found[6] that for the IHM, treated within single site DMFT, the band gap becomes zero at a critical U_{c1}, with a Mott gap re-emerging at a larger U_{c2}. In between, the system is metallic. A subsequent cluster DMFT study of Kancharla *et al.*[7] which incorporated antiferromagnetic correlations, found a phase diagram with somewhat different topology, but still exhibiting an intermediate region which was suggested to have bond ordered wave character.

Model: In this paper, we shall consider a bilayer Hubbard Hamiltonian:

$$
\begin{aligned}
\hat{\mathcal{H}} = &-\sum_{\langle \mathbf{jk}\rangle,l,\sigma} t_l (c^\dagger_{\mathbf{j},l,\sigma} c_{\mathbf{k},l,\sigma} + c^\dagger_{\mathbf{k},l,\sigma} c_{\mathbf{j},l,\sigma}) \\
&-V\sum_{\mathbf{j},\sigma}(c^\dagger_{\mathbf{j},1,\sigma} c_{\mathbf{j},2,\sigma} + c^\dagger_{\mathbf{j},2,\sigma} c_{\mathbf{j},1,\sigma}) - \sum_{\mathbf{j},l,\sigma}\mu_l n_{\mathbf{j},l,\sigma} \\
&+U\sum_{\mathbf{j},l}(n_{\mathbf{j},l,\uparrow} - \tfrac{1}{2})(n_{\mathbf{j},l,\downarrow} - \tfrac{1}{2})
\end{aligned}
\tag{1}
$$

which provides a specific realization of the effect of electronic correlation in band insulators. In Eq. 1, $c^\dagger_{\mathbf{j},l,\sigma}(c_{\mathbf{j},l,\sigma})$ are creation(destruction) operators for fermions of spin σ on site $\mathbf{j}$ of layer $l = 1, 2$. The intralayer hoppings are t_l between near-neighbor sites $\mathbf{j}, \mathbf{k}$ of a two dimensional square lattice, and the interlayer hopping is V. Correlation is introduced in the model through the on-site repulsion U. We have included a chemical potential μ_l for generality. However, here we focus on the half-filled case $\mu_l = 0$.

If the in-plane hoppings are chosen with opposite sign, $t_1 = -t_2 \equiv t$, Eq. 1 is a band insulator at $U = 0$ with

$E_{\mathbf{q}} = \pm\sqrt{\epsilon_{\mathbf{q}}^2 + V^2}$. (In the remainder of this paper $t = 1$ will be taken as the unit of energy.) This bears a strong resemblance to the dispersion relation of the 2D IHM whose superlattice potential $\Delta \sum_{\mathbf{j}}(-1)^{\mathbf{j}} n_{\mathbf{j}}$ similarly has the effect of opening a band gap at $\mathbf{q} = (\pi, \pi)$, altering the $\Delta = 0$ dispersion relation $\epsilon_{\mathbf{q}}$ to $E_{\mathbf{q}} = \pm\sqrt{\epsilon_{\mathbf{q}}^2 + \Delta^2}$. Real space Quantum Monte Carlo (QMC)[8] has supplemented DMFT studies of the IHM[6] by allowing for magnetic order and concluded that U could cause the appearance of a metallic phase. However, despite the similarity in $E_{\mathbf{q}}$ between the IHM and Eq. 1, the physics of the two models is fundamentally different: the bilayer has twice as many allowed $\mathbf{q}$ points and uniform average density, $\langle n_{\mathbf{j},l,\sigma} \rangle = \frac{1}{2}$. This is in contrast to the staggered charge density wave pattern in the presence of the superlattice potential in the IHM. This difference, combined with the local character of the interaction, is at the origin of the contrast in the ground state properties which we will present.

As with the IHM, the Hamiltonian in Eq. 1 has been previously studied within the DMFT formalism [9], with a model hybridizing two bands with identical, semi-elliptical density of states. DMFT finds a scenario remarkably similar to the one observed for the metal-insulator case in the standard single band model at half-filling: a first order transition between band and Mott insulator characterized by a discontinuous change in the double occupancy. Remarkably, upon increasing the interaction, DMFT also predicts that the single-particle gap should monotonically shrink in stark contrast with the behavior in the Mott phase where the gap grows monotonically with U.

We will explore these issues using determinant Quantum Monte Carlo (DQMC) [10]. This method allows an exact calculation[11] of the properties associated to the Hamiltonian in Eq. 1, on lattices of finite spatial extent. Here we will show results for systems consisting of two sheets of up to $N = 14 \times 14$ sites.

Magnetic transition: We start our discussion of the phases of Eq. 1 by looking for possible antiferromagnetic long-range order (LRO). The most direct signature is the thermodynamic extrapolation of the in-layer structure factor (which has the same value on the two layers),

$$S(\mathbf{q}) = \frac{1}{6N} \sum_{\mathbf{j},\mathbf{k},l} \langle \sigma_{\mathbf{k},l}^z \sigma_{\mathbf{j},l}^z + 2\, \sigma_{\mathbf{k},l}^- \sigma_{\mathbf{j},l}^+ \rangle\, e^{i\mathbf{q}\cdot(\mathbf{k}-\mathbf{j})} \quad (2)$$

$$\sigma_{\mathbf{j}}^z = c_{\mathbf{j}\uparrow}^\dagger c_{\mathbf{j}\uparrow} - c_{\mathbf{j}\downarrow}^\dagger c_{\mathbf{j}\downarrow}; \quad \sigma_{\mathbf{j}}^+ = c_{\mathbf{j}\uparrow}^\dagger c_{\mathbf{j}\downarrow}; \quad \sigma_{\mathbf{j}}^- = c_{\mathbf{j}\downarrow}^\dagger c_{\mathbf{j}\uparrow}$$

converging to a non-zero value as $N \to \infty$. We will focus on antiferromagnetism, $S^{\text{af}} = S(\pi, \pi)$, which is the expected dominant magnetic instability at half-filling. Because of the continuous spin symmetry and the fact that we are in two dimensions, we expect LRO only at $T = 0$.

The finite size scaling analysis necessary to locate the critical value of U for onset of magnetic order is presented
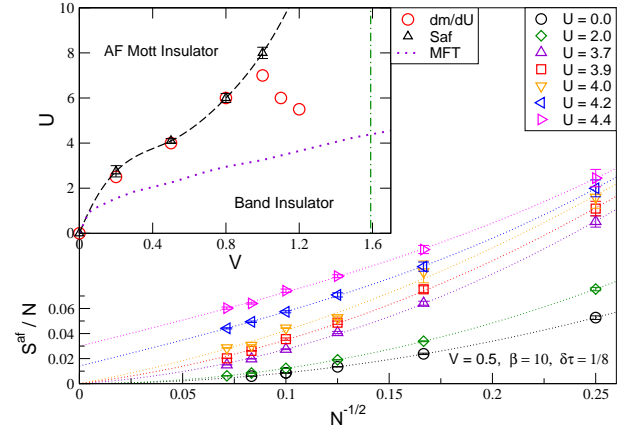

FIG. 1: Finite-size scaling of the AF structure factor at $V = 0.5$. Symbols are DQMC data for S^{af}. Lines are fits to third-order polynomials in the inverse linear lattice size $1/\sqrt{N}$. The inset shows the transition line computed with DQMC (dashed) and MFT (dotted). The vertical line corresponds to the critical V, predicted by studies on the Heisenberg model, above which no magnetic long order is possible. Circles correspond to maxima in dm/dU as a function of U at constant V (see Fig. 2).

in Fig. 1 for $V = 0.5$. At weak coupling $U \lesssim 4.0$ there is no LRO. As the on-site repulsion increases, LRO sets in around $U \approx 4.2$. Our value of U_c is significantly smaller than the DMFT estimate of approximately 5.5 [9] which was however computed for a transition to a Mott insulating state without long range magnetic order.

We repeated the finite size scaling analysis for several other values of V and obtained the phase diagram shown in the inset of Fig.1. There is a qualitative difference between the DQMC results and the transition line mean field theory (MFT) predicts. Beyond $V = 0.5$ the DQMC curves rises much more sharply than the MFT one as a result of the competition between interplanar singlet formation and AFM correlation which is lacking in the mean-field description. Note also that known results for the Heisenberg bilayer[12, 13] imply that for $V > V_c = 1.59$, no order is established regardless of the magnitude of U. Determining the values of U_c as V_c is approached becomes quickly intractable for $V > 1.0$ since the energy scale at which magnetic correlations develop decreases and fluctuations in the DQMC measurements of long range correlations increase.

Local moments: Within DMFT[9], the phase boundary is determined by a discontinuity in the double occupancy d, the latter being related to the local moment m by,

$$m = \frac{1}{N} \sum_{\mathbf{j}} \langle (\sigma_{\mathbf{j}}^z)^2 \rangle = 1 - \frac{2}{N} \sum_{\mathbf{j}} \langle n_{\mathbf{j}\uparrow} n_{\mathbf{j}\downarrow} \rangle = 1 - 2d.$$

Local moment formation is the key signature for the onset of Mott insulating behavior and it has been previously reported to happen discontinuously at a Mott metal-
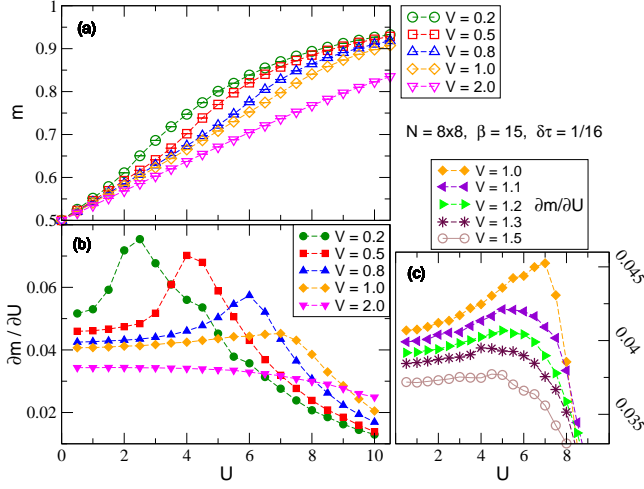
FIG. 2: (a) Local moment m as a function of U for 8×8 layers at $\beta = 15$ (symbols). (b) first derivative of the local moment with respect to U, $\partial m/\partial U$, shows a peak at the transition to the Mott insulating state. (c) A close up view of (b) shows the peak is no longer present for any U above $V_c \approx 1.2$.
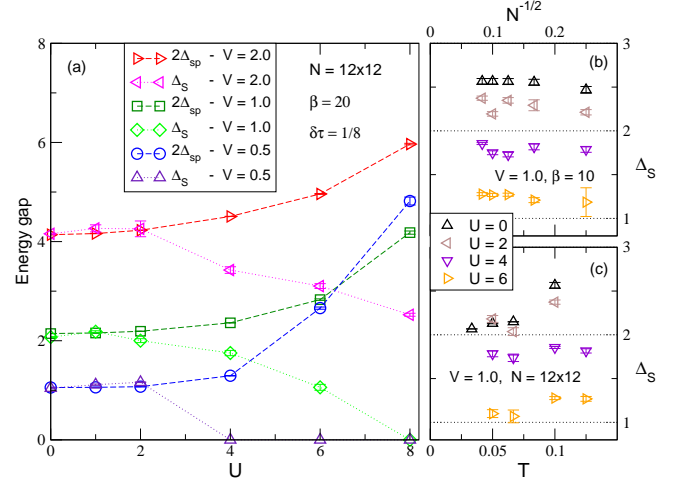
FIG. 3: Main panel: Gaps in the single particle spectral function and the spin-spin correlation function are shown as functions of interaction U for several values of interlayer hopping V. At weak U, the spin gap Δ_S is precisely twice the single particle gap Δ_{sp}, as expected in a Fermi liquid phase. The smaller panels at right show the finite size (top) and finite temperature (bottom) effects for the spin gap.

insulator transition within other approaches as well, such as path-integral renormalization group [14] and variational Monte Carlo [15]. Figure 2a shows the dependence of m on interaction strength for several values of V with no evidence of the sharp discontinuity found in DMFT.

However, for small V (e.g. $V = 0.5$), we found that the magnetic transition is located in correspondence to a maximum in $\partial m/\partial U$ (see Fig. 2b). Numerical differentiation does not allow us to establish whether there is an actual singularity in the behavior of $\partial m/\partial U$ — so that one could use this quantity to characterize a phase transition — or whether the maximum is a simple manifestation of a cross over to the local moment regime. At larger V the value of U where the maximum appears is reduced (Fig. 2c and circles in Fig.1), presumably as a consequence of the increased electron localization on the interplane bonds, whereas U_c for the onset of AFLRO is expected to grow monotonically. This decoupling of the behavior of local moments from magnetism is suggestive of the possibility of an intervening Mott insulating state with no broken symmetries.

Energy gaps and spectral functions: We now investigate the evolution of the energy spectra. The single-particle gap Δ_{sp} and spin excitation gap Δ_S were extracted from the imaginary time-dependent correlations

$$G(\tau) = \sum_{\mathbf{i},\sigma} \langle c_{\mathbf{i},\sigma}(\tau) c_{\mathbf{i},\sigma}^\dagger(0) \rangle \propto e^{-\tau\Delta_{sp}}$$

$$\chi(\tau) = \sum_{\mathbf{i},\sigma} \langle \sigma_{\mathbf{i},\sigma}^z(\tau) \sigma_{\mathbf{i},\sigma}^z(0) \rangle \propto e^{-\tau\Delta_S}.$$

Figure 3a shows the evolution of these gaps when the interaction U is increased, for different values of the inter-

layer hybridization V. Starting from the non-interacting limit, where the single-particle gap and the spin gap are expected to be respectively equal to V and $2V$, the two quantities follow opposite evolutions regardless of whether there is a tendency toward AFM (small V) or singlet formation (large V). In particular, we found that for all three values of V considered in Fig. 3, the effect of correlation is negligible up to $U \simeq 2$, in agreement with the findings of Sentef [9]. However, we observe a significant discrepancy between the effect of correlation in DMFT and in DQMC: in DQMC the single particle gap Δ_{sp} shows no indication of the shrinking trend predicted by DMFT, not even in the small U limit where the role of long range correlation should be negligible and the paramagnetic solution is likely the correct ground state within single-site DMFT. We checked that the values of the gaps are converged in both size of the cluster (Fig. 3b) and temperature (Fig. 3c). Although it is certainly the case that this difference in physics is associated with the effects of non local spatial correlations on spectral properties, as noted in discussions of cluster extensions of DMFT[16–18], our calculation does not allow to address the interesting issue of whether the discrepancy originates from the neglect of interlayer singlet correlation or intralayer short-range anti-ferromagnetism. The former represents a somewhat more severe failure of single-site DMFT as the difference would be largely independent of the underlying lattice structure and on whether or not the latter supports any ordering tendencies.

In-layer momentum-resolved single-particle and spin excitation spectra ($A(\mathbf{q},\omega)$ and $\chi(\mathbf{q},\omega)$) are obtained by
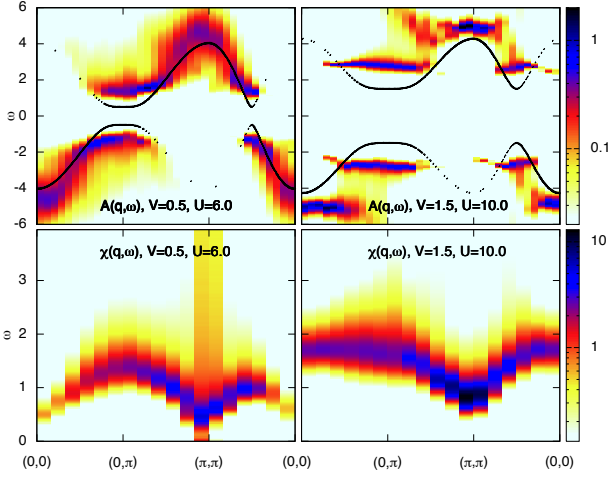
FIG. 4: Top row: single particle spectral function in the presence(left) and absence (right) of AFM order. Bottom row: same as top row but for the spin spectral function. Results are computed on a $N = 12 \times 12$ cluster at $\beta = 20$. Lines in the top panels are the corresponding energy bands when $U = 0$.

inverting the integral equations

$$G(\mathbf{q}, \tau) = \int_0^\beta A(\mathbf{q}, \omega) \frac{e^{-\omega\tau}}{1 + e^{-\beta\omega}} d\omega$$

$$\chi(\mathbf{q}, \tau) = \int_0^\beta \chi(\mathbf{q}, \omega) \frac{e^{-\omega\tau}}{1 - e^{-\beta\omega}} d\omega.$$

using the maximum entropy method [19, 20]. $G(\mathbf{q}, \tau)$ and $\chi(\mathbf{q}, \tau)$ are the in-layer momentum resolved counterparts of the correlation functions previously introduced. Figure 4 shows the single-particle (top panels) and spin (bottom panels) spectral densities and compare an AFM situation (left) against a case where no order is found by a finite size scaling analysis(right). Thanks to the Goldstone theorem, the spin spectra provide a complementary indication of the presence or lack of AFM long range order. We verified that, indeed, parameter regimes that were predicted to be AFM by scaling analysis are characterized by the existence of a massless mode at (π, π) which is conspicuously absent in paramagnetic cases. The single particle spectrum, on the other hand, helps in characterizing the paramagnetic phase more precisely as it shows an almost rigid shift of the non-interacting bands, a behavior indicative of a Mott insulating regime. At large V, but still below V_c, our results therefore suggest that, upon increase of U, the system shows a first crossover to a featureless Mott insulating state and then a transition into the anti-ferromagnet. It is the crossover that can be most directly contrasted with the DMFT scenario which predicts a split narrowing resonance in the weak-to-intermediate U range and then a transition to a Mott insulator.

Spin correlations: The real space spin correlations across the layers $\langle \sigma_{\mathbf{j}1} \cdot \sigma_{\mathbf{j}2} \rangle$ are shown in Fig. 5a. The generic

behavior of bilayer models (and related Hamiltonians like the periodic Anderson model) is the development of singlets with increasing V at fixed U, and the associated destruction of AFLRO, signalled by a growth in $\langle \sigma_{\mathbf{j}1} \cdot \sigma_{\mathbf{j}2} \rangle$. The development of such interplane spin correlations can be seen in Fig. 5 by comparing the different curves at fixed U. The evolution at fixed V also provides consistent indications of the underlying physics previously inferred from the structure factor S^{af}, the local moment m, and the excitation gaps. Specifically, the interlayer spin correlations first increase as interactions are turned on, but then have a kink, or even turn over, as the AF phase is entered. For $V = 0.5$ for example, the kink appears at $U \approx 4.0$.

The intra-plane real space nearest-neighbor spin correlations are shown in panel (b) of Fig. 5. They increase monotonically (in absolute value) with U for all V, indicating that the on-site Hubbard U enhances short range intraplane antiferromagnetism[21]. This quantity offers yet another local diagnostic for the onset of order as it shows an inflection point in close correspondence to the transition. Moreover, comparison of the results in the two panels at $V = 0.5$ and small U reveals that it is the interplane spin correlation that grows more rapidly. We take this as a further indication that the discrepancy in the behavior of the single particle gap between our calculation and single site DMFT is not due to the presence of intralayer short-ranged magnetic order but to the inclusion, by the DQMC approach used here, of interlayer singlet correlations.
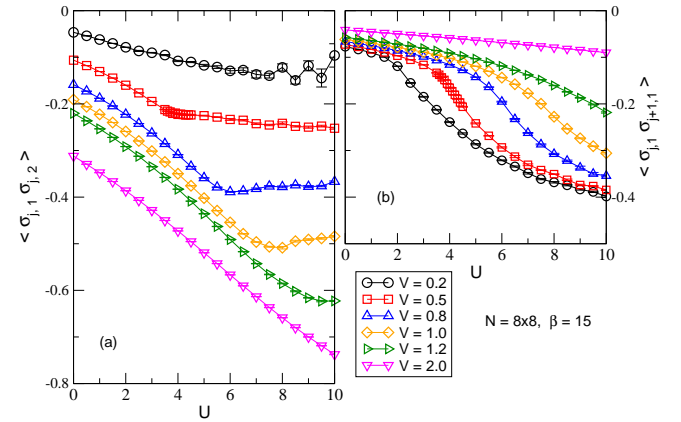

FIG. 5: Near-neighbor real space spin-spin correlations (a) across the layers and (b) within an individual plane. At small $V < 1.2$ the correlations converge to finite values characterizing the magnetic ordered phase, while for large $V = 2.0$, the system is made of almost decorrelated singlets.

Conclusions: In this paper we studied the effect of introducing local interaction in the band insulator formed by a bilayer with opposite sign of the hopping integral. We found strikingly different physics from the ionic Hub-

bard model owing to the fact that the system is perfectly homogeneous and accompanied by a tendency toward singlet formation as the band gap increases. As the strength of the interaction is increased, and below a critical interplane hybridization, a transition to a Mott insulator with antiferromagnetic order ensues. This transition was studied by examining several physical observables such as the magnetic structure factor, the local moments, single-particle and spin excitations resolved in both energy and momentum, and spin correlations. The behavior of $\partial m/\partial U$ and spectral functions suggests that, as V grows, the magnetic transition is preceeded by a cross-over into a featureless Mott insulating state. A more subtle question is whether such cross-over may, in fact, be a transition. Obviously, this is a delicate point that requires validation from calculations on larger clusters and the use of a direct estimator for $\partial m/\partial U$ rather than the finite difference employed in this work.

———————

[1] "Disordered Electronic Systems," P.A. Lee and T.V. Ramakrishnan, Rev. Mod. Phys. **57**, 287 (1985).

[2] "The Anderson-Mott transition," D. Belitz and T. R. Kirkpatrick, Rev. Mod. Phys. **66**, 261 (1994).

[3] "Conductor-Insulator Quantum Phase Transitions", edited by V. Dobrosavljevic, N. Trivedi, and J. Valles; Oxford University Press (2012).

[4] J. Hubbard and J.B. Torrance, Phys. Rev. Lett. **47**, 1750 (1981).

[5] A. Georges, G. Kotliar, W. Krauth, and M.J. Rozenberg , Rev. Mod. Phys. **68**, 13 (1996).

[6] A. Garg, H.R. Krishnamurthy, and M. Randeria, Phys. Rev. Lett. **97**, 046403 (2006).

[7] S.S. Kancharla and E. Dagotto, Phys. Rev. Lett. **98**, 016402 (2007).

[8] N. Paris, K. Bouadim, F. Hebert, G.G. Batrouni, and R.T. Scalettar, Phys. Rev. Lett. **98**, 046403 (2007).

[9] M. Sentef, J. Kunes, P. Werner and A. P. Kampf, Phys. Rev. **B80**, 155116 (2009).

[10] R. Blankenbecler, D.J. Scalapino and R.L. Sugar, Phys. Rev. **D24**, 2278 (1981).

[11] The only approximation is the introduction of a finite discretization of the inverse temperature $\beta = 1/T = L\Delta\tau$. The resulting 'Trotter errors' can be eliminated through an extrapolation to $\Delta\tau = 0$. For the $\Delta\tau$ values chosen here, we have verified that such an extrapolation does not shift the physical results significantly.

[12] K. Hida, J. Phys. Soc. Jpn. **61**, 1013 (1992).

[13] L. Wang, K.S.D. Beach and A.W. Sandvik, Phys. Rev. **B73**, 014431 (2006).

[14] T. Kashima and M. Imada, J. Phys. Soc. Jpn. **70**, 3052 (2001).

[15] D. Tahara and M. Imada, J. Phys. Soc. Jpn. **77**, 093703 (2008).

[16] T. Maier, M. Jarrell, Th. Pruschke, and M.H. Hettler Rev. Mod. Phys. **77**, 1027 (2005).

[17] H. Hafermann, G. Li, A.N. Rubtsov, M.I. Katsnelson, A.I. Lichtenstein, and H. Monien, Phys. Rev. Lett. **102**, 206401 (2009).

[18] A.A. Katanin, A. Toschi, and K. Held, Phys. Rev. **B80** 075104 (2009).

[19] J.E. Gubernatis, M. Jarrell, R.N. Silver, and D.S. Sivia, Phys. Rev. **B44**, 6011 (1991).

[20] K.S.D. Beach, arXiv preprint cond-mat/0403055 (2004).

[21] For fixed non-zero T, the spin correlations would ultimately go down as U increases owing to the $1/U$ dependence of J. In Fig. 5, however, since $\beta = 15$ we are sufficiently close to the ground state not to observe that effect.